



Mapping wildfire and clearcut harvest disturbances in boreal forests with Landsat time series data

Todd A. Schroeder^{a,*}, Michael A. Wulder^b, Sean P. Healey^a, Gretchen G. Moisen^a

^a U.S. Department of Agriculture Forest Service, Rocky Mountain Research Station, 507 25th St., Ogden, UT 84401, USA

^b Canadian Forest Service (Pacific Forestry Centre), Natural Resources Canada, 506 West Burnside Rd., Victoria, British Columbia V8Z 1M5, Canada

ARTICLE INFO

Article history:

Received 22 May 2010

Received in revised form 26 January 2011

Accepted 29 January 2011

Available online 12 March 2011

Keywords:

Forest disturbance mapping

Wildfire

Clearcut harvest

Landsat time series

Image classification

Monitoring

ABSTRACT

Information regarding the extent, timing and magnitude of forest disturbance are key inputs required for accurate estimation of the terrestrial carbon balance. Equally important for studying carbon dynamics is the ability to distinguish the cause or type of forest disturbance occurring on the landscape. Wildfire and timber harvesting are common disturbances occurring in boreal forests, with each having differing carbon consequences (i.e., biomass removed, recovery rates). Development of methods to not only map, but distinguish these types of disturbance with satellite data will depend upon an improved understanding of their distinctive spectral properties. In this study, we mapped wildfires and clearcut harvests occurring in a Landsat time series (LTS) acquired in the boreal plains of Saskatchewan, Canada. This highly accurate reference map ($\kappa = 0.91$) depicting the year and cause of historical disturbances was used to determine the spectral and temporal properties needed to accurately classify fire and clearcut disturbances. The results showed that spectral data from the short-wave infrared (SWIR; e.g., Landsat band 5) portion of the electromagnetic spectrum was most effective at separating fires and clearcut harvests possibly due to differences in structure, shadowing, and amounts of exposed soil left behind by the two disturbance types. Although SWIR data acquired 1 year after disturbance enabled the most accurate discrimination of fires and clearcut harvests, good separation (e.g., $\kappa \geq 0.80$) could still be achieved with Landsat band 5 and other SWIR-based indices 3 to 4 years after disturbance. Conversely, minimal disturbance responses in near infrared-based indices associated with green leaf area (e.g., NDVI) led to unreliably low classification accuracies regardless of time since disturbance. In addition to exploring the spectral and temporal manifestation of forest disturbance types, we also demonstrate how Landsat change maps which attribute cause of disturbance can be used to help elucidate the social, ecological and carbon consequences associated with wildfire and clearcut harvesting in Canadian boreal forests.

Published by Elsevier Inc.

1. Introduction

Over 75% of Canada's roughly 400 million ha of forest and woodland are classified as boreal forest (Brandt, 2009). Boreal forests are subject to frequent natural (e.g., fire, insect and wind) and anthropogenic (e.g., industrial development, land use change and harvesting) disturbance events (Wulder et al., 2009a), which can lead to considerably different ecological effects (Niemelä, 1999). Fire is the primary disturbance agent in the region (Heinselman, 1983; Weber & Flannigan, 1997) with return intervals typically around 50 to 150 years (Payette, 1992). Shifts in fire regime between the 1960s–70s and the 1980s–90s resulted in a doubling of annual burned area and more than double the frequency of large fire events (Kasischke & Turetsky, 2006). Over the past 30 years, the high latitudes of North

America have experienced a 1.5 to 2.0 °C rise in temperature (Easterling et al., 2000). Studies have shown that in some boreal ecozones, fire cycles are well correlated with growing season temperatures and precipitation anomalies (Skinner et al., 1999; Zhang & Chen, 2007), leading some to suggest that increased warming is contributing to the increased frequency and severity of fires (Gillett et al., 2004). Despite increases in frequency and severity, wildfires are an integral component of Canadian boreal ecosystems (Wulder et al., 2007), with many tree species requiring fire to prepare the soil and/or encourage seeding.

In addition to fire, roughly one quarter of Canada's boreal forest area is managed for industrial wood production. Like fire frequency, harvesting levels (in terms of area) have also increased over recent decades (Government of Canada, 1995, 2008), with a drop evidenced around 2006 coinciding with a decline in global economic activity. Harvesting rates are generally governed by an annual allowable cut of 1% of area eligible for harvest. In the boreal plains ecozone for example, the annual area of land harvested increased by 125% between 1975 and 1993 (Government of Canada, 1996) as new, previously unaccessed

* Corresponding author. Tel.: +1 801 625 5040; fax: +1 801 625 5723.

E-mail addresses: tschroeder@fs.fed.us (T.A. Schroeder),

mwulder@pfc.cfs.nrcan.gc.ca (M.A. Wulder), seanhealey@fs.fed.us (S.P. Healey),

gmoisen@fs.fed.us (G.G. Moisen).

areas, were opened for harvesting. Although selection harvesting methods are being used more frequently across Canada, clearcut harvesting has been and continues to be the dominant harvesting practice (Fricker et al., 2006), as it is most appropriate for emulation of natural processes and to encourage self-seeding and regeneration (Perera et al., 2004; Wulder et al., 2007). It is estimated that 88% of the approximately 42 million ha of timber harvested in Canada between 1920 and 1996 were clearcut (Government of Canada, 1995, 2008). While harvesting is limited by regulation, wildfires – especially in the northern boreal – burn without suppression and can vary markedly in area burned. In more southern managed areas of the boreal, fire suppression is common to protect forest resources and co-located communities.

Although fires and clearcuts both result in tree mortality and loss of biomass, each impacts the landscape at different scales, frequencies, and levels of intensity, ultimately leading to different patterns of landscape structure (e.g., patch size and shape, Gluck & Rempel, 1996; Schroeder & Perera, 2002) and vegetation regrowth (e.g., species composition, Ilisson & Chen, 2009). Given the large land area affected by fire and harvesting, it is not surprising that disturbance dynamics have been identified as one of the key drivers of the net carbon balance in forests (Goetz et al., 2009; Harmon, 2001; Kurz & Apps, 1999; Kurz et al., 2009). As each disturbance type impacts the carbon cycle in different ways (Mkhabela et al., 2009), it is important that effects from human action are separated from those of natural origin (Birdsey et al., 2007). As a result, maps that attribute forest disturbance to fire or clearcut harvest would improve estimates of carbon lost to the atmosphere, as well as facilitate the tracking of carbon gained by vegetation recovery.

Recent advances in satellite mapping technology have led to the development of algorithms which can track and characterize forest disturbances at continental and global scales. For example, the MODerate-resolution Imaging Spectroradiometer (MODIS) global disturbance index (MGDI; Mildrexler et al., 2007) uses 1 km spatial resolution Land Surface Temperature (LST) and Enhanced Vegetation Index (EVI) data from MODIS to detect broad scale forest disturbances resulting from fire, insect infestation and hurricanes (Mildrexler et al., 2009). The MODIS burned area algorithm (Giglio et al., 2009) combines 500 m MODIS reflectance imagery with 1 km MODIS active fire observations to produce automated monthly estimates of burned area for the global land surface (MODIS MCD45 burned area product; Giglio et al., 2009; Roy et al., 2005). Although the global disturbance index can accurately detect a variety of forest disturbances which occur over large areas (see Coops et al., 2009), the type of disturbance is not automatically attributed. The MODIS burned area product has also proven accurate; however, the 1 km pixels limit the minimum detectable size of disturbance, often leading to high rates of omission error (Roy & Boschetti, 2009). In addition, disturbance products developed with coarse resolution imagery are less capable of detecting small scale disturbances such as those from forest harvesting activities (Wulder et al., 2009a).

Another option for mapping historical forest disturbances from fire and clearcutting is through the use of the Landsat archive of optical satellite images (Cohen & Goward, 2004). In addition to being systematically collected and consistently calibrated, Landsat data are well suited for studying vegetation disturbance dynamics as information is collected in a number of important spectral wavelengths (e.g., visible, near-infrared and shortwave-infrared) with a pixel size (28.5 m) capable of resolving most disturbance types (e.g., natural and anthropogenic) which occur in forest systems (Townshend & Justice, 1988; Wulder et al., 2008). The recent free release of the Landsat archive (Woodcock et al., 2008) has eliminated the prohibitive costs of assembling long image time series and has resulted in an increase in the development of automated algorithms (Huang et al., 2010a; Kennedy et al., 2007) which are capable of detecting changes in forest cover over large temporal and spatial extents.

Despite this progress, however, little work has gone into identifying signal characteristics which might ultimately support automated labeling of the causes of mapped disturbances. There have been LTS-based maps separating different disturbance causes (e.g., Healey et al., 2008), but classification decision rules have been empirical and ad hoc. Our objective is to determine if the physical changes resulting from fire and clearcut harvesting yield sufficiently distinct spectral patterns to allow for accurate classification through time. This improved understanding will ultimately support the development of more automated disturbance labeling protocols for disturbance type (e.g., fire, harvest) from the spectral trends present in Landsat time series.

To address our objectives we use a near-annual, 16 image (22 year) Landsat time series (LTS) located in the boreal plains ecozone of central Saskatchewan, Canada. An analyst driven, multi-temporal RGB color composite change detection approach (Sader & Winne, 1992; Wilson & Sader, 2002) is used to map both year and type of forest disturbance. An independent, design-based accuracy assessment based on visual interpretation of LTS data is used to determine the accuracy of the disturbance map. Once validated, the disturbance map is used to conduct an iterative classification test aimed at determining how spectral wavelength and time since disturbance impact the spectral discrimination of fire and clearcut disturbances. Using six Landsat bands and indices associated in the literature with either forest structure (e.g., short-wave infrared reflectance) or green leaf area (e.g., vegetation indices such as NDVI), we determine the time interval required to accurately classify the two disturbance types using images acquired 1 to 10 years after disturbance. We conclude by highlighting potential applications of LTS disturbance maps which attribute cause of disturbance, such as linking forest policy to harvesting rates, estimating burned area and tracking rates of post-disturbance vegetation recovery.

2. Methods

2.1. Study area

The study area is located in central Saskatchewan (Fig. 1) within the 740,000 km² Boreal Plains ecozone, one of 15 terrestrial ecozones in Canada (Marshall & Schut, 1999). The area is characterized by moderate topography, with elevation ranging from 600 to 760 m. Nearly 84% of the land surface is forested, with white spruce (*Picea glauca*), black spruce (*Picea mariana*), jack pine (*Pinus banksiana*), and tamarack (*Larix laricina*) making up the primary main stand conifer species in this region. There is also a wide distribution of broadleaf trees, particularly white birch (*Betula papyrifera*), trembling aspen (*Populus tremuloides*), and balsam poplar (*Populus balsamifera*). Soils are characteristically dark gray and gray luvisols, which tend to form under the mixed-wood and conifer forests of the region (Morrison & Kraft, 1994). In poorly drained areas, peat bogs are common. Precipitation is about 400 mm over much of the ecozone, nearing 500 mm along the southern boundary. The mean daily January temperature ranges from −17.5 °C to −22.5 °C, with the mean daily July temperature ranging from 12.5 °C to 17.5 °C (Lands Directorate, 1986).

2.2. Landsat time series (LTS)

The LTS consists of 16 growing season (May–September), Landsat TM and ETM+ images (WRS-2, path 37 row 22) (Table 1). The majority of images fall on an annual time step (i.e., one image per year) with the longest gap between successive images being two years. The images, at a spatial resolution of 28.5 m, were ortho-rectified and converted to surface reflectance using the Landsat Ecosystem Disturbance Adaptive Processing System (LEDAPS, Masek et al., 2006). To minimize unwanted spectral variability resulting from seasonal sun-surface-sensor view angle effects each image was normalized to a common radiometric

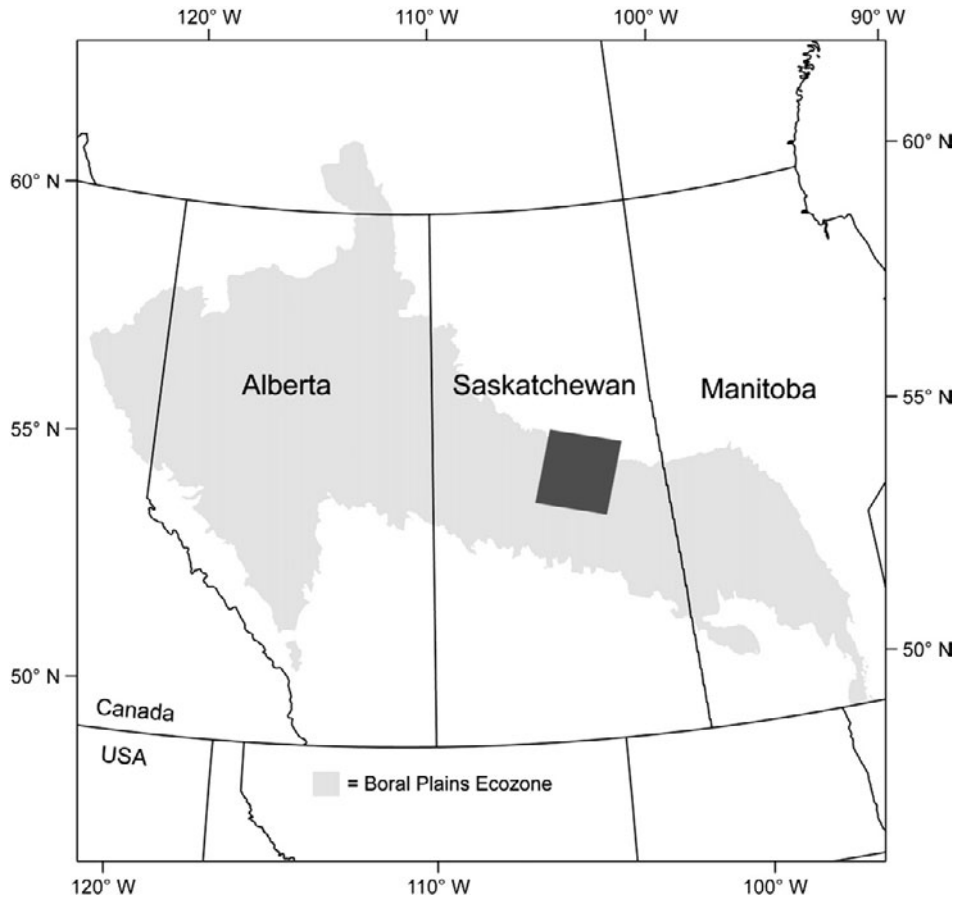


Fig. 1. Location of Landsat path 37 row 22 study area in the boreal plains ecozone, Canada.

reference image (the 1987 image in this case). Pseudo-invariant features (i.e., pixels with stable reflectance over time) located with the iteratively re-weighted Multivariate Alteration Detection (MAD) algorithm (Canty & Nielsen, 2008) were used in conjunction with reduced major axis regression (Cohen et al., 2003; Larsson, 1993) to match the individual spectral bands of each image to the reference scene (Schroeder et al., 2006). Masks of cloud and cloud shadow were derived with the algorithm of Huang et al. (2010b). The identified areas were then filled using a temporal interpolation approach which estimates spectral values using the temporally nearest pixel observations acquired before and after the cloudy observations (see Eq. 5, Huang et al., 2010a).

2.3. Spectral bands/indices

Six Landsat spectral bands/indices commonly used in the ecological remote sensing of forest environments (Cohen & Goward, 2004) are used to determine how spectral wavelength and time since disturbance impact the classification of fire and clearcut disturbances. The selected bands/indices fall into two general groups according to their sensitivity to either forest structure or green leaf area. Consisting of bands/indices primarily derived from short-wave infrared (SWIR) reflectance, the forest structure group includes 1) Landsat band 5 (B5), which is acquired directly by the Landsat sensor in the mid-infrared spectral region (1.55–1.75 μm), 2) Tasseled Cap Wetness (Crist & Cicone, 1984), which is the third component of a guided principal component transformation representing a contrast of TM bands 5 and 7 with the other four TM bands (based here on the reflectance transformation of Crist, 1985); and, 3) the forestness index (FI, Huang et al., 2008, 2009, 2010a), which is an integrated z-score measure of a pixels likelihood of being forested, calculated with TM bands 3, 5 and 7 as:

$$FI_p = \sqrt{\frac{1}{NB} \sum_{i=1}^{NB} \left(\frac{b_{pi} - \bar{b}_i}{SD_i} \right)^2} \quad (1)$$

where \bar{b}_i and SD_i are the mean and standard deviation of forest training pixels within an image for band i , b_{pi} is the band i spectral value for pixel p , and NB is the number of spectral bands. In forested environments both B5 and Wetness have been found to be sensitive to vegetation density and structure, shadowing, and leaf moisture content (Crist & Cicone, 1984; Horler & Ahern, 1986). In boreal forests of Russia, B5 has been shown to effectively discriminate clearcut, fire

Table 1
The Path 37 row 22 Landsat time series (LTS).

Sensor	Date
TM	5/23/1986
TM	8/30/1987
TM	9/4/1989
TM	8/22/1990
TM	9/10/1991
TM	6/27/1993
TM	9/1/1994
TM	6/17/1995
TM	9/10/1997
TM	8/28/1998
ETM	7/22/1999
ETM	8/12/2001
TM	8/23/2002
TM	8/12/2004
TM	9/3/2006
TM	9/24/2008

and insect disturbance classes (Ranson et al., 2003), while Wetness has been previously shown to be insensitive to topographically induced illumination angle (Cohen & Spies, 1992). FI is an inverse measure of the likelihood a pixel is forested, thus an FI value close to zero indicates a pixel is close to the spectral value of undisturbed forest, while high FI values indicates a pixel is likely non-forest. FI is sensitive to forest structure and has also proven useful for detecting forest change without prior knowledge of forest type (i.e., conifer vs. deciduous) (Huang et al., 2010a).

The green leaf area group, consisting of indices derived primarily from near-infrared (NIR) reflectance, includes 4) normalized difference vegetation index (NDVI, Rouse et al., 1973), which is a ratio of measured red and NIR reflectance calculated as: $(TM4 - TM3)/(TM4 + TM3)$, 5) normalized burn ratio (NBR, Key & Benson, 2005), which is a ratio of mid-infrared and NIR reflectance calculated as: $(TM4 - TM7)/(TM4 + TM7)$, and 6) Tasseled Cap angle (TCA, Powell et al., 2010), a new transformation calculated as: $\arctan(\text{Tasseled Cap Greenness}/\text{Tasseled Cap Brightness})$. NDVI has been found to be sensitive to the vigor and density of green vegetation, leaf area, and the fraction of photosynthetically active radiation absorbed by plant canopies (Sellers et al., 1992). In sparsely vegetated areas NDVI has been shown to be highly influenced by background soil material (Huete, 1988) and in densely forested areas NDVI has been shown to reach a saturation point (Asrar et al., 1984; Turner et al., 1999), with estimation of $LAI \geq 4$ often becoming imprecise (Baret & Guyot, 1991; Running et al., 1986). Widely used to estimate burn severity (Eidenshink et al., 2007), NBR is primarily sensitive to living chlorophyll, moisture content of leaves and soils, and char and ash (Elvidge, 1990; Key, 2006). It has been shown to be negatively impacted by topographic effects (Verbyla et al., 2008) leading some to question whether NBR is consistently sensitive to various levels of fire severity (French et al., 2008; Roy et al., 2006; Wulder et al., 2009b). Although personal observations have led the authors to believe TCA behaves similarly to NDVI, it has not been well studied, thus we include it here as a means of better understanding its response to fire and clearcut disturbance. Further, TCA offers an additional benefit of offering a spectral bridge between Landsat MSS (which does not contain SWIR bands) and the later TM and ETM+ series of sensors in support of time series based investigations (that is, prior to the July 6, 1982 launch of Landsat-4 back to the July 23, 1972 launch of Landsat-1).

2.4. Canadian Large Fire Database

Data on forest fires collected by provincial, territorial and other federal agencies across Canada have been compiled into the Canadian Large Fire Database (LFDB, Amiro et al., 2001; Stocks et al., 2003). The initial effort compiled reliable data on forest fires (excluding rangelands) greater than 200 ha occurring between 1959 and 1999, with later mapping efforts utilizing satellite observations (see Fraser et al., 2004). The database includes information on fire ignition date, area burned, suppression efforts, cause of ignition and mapped spatial location, including both point and polygon GIS layers. Efforts have been made since the initial compilation of the data set to update it both backward and forward in time, resulting in the version used here which includes fires occurring from 1917 to 2006. Based on the fire perimeter data, the study area contains more than 30 fires (6 with partial coverage) dating between 1980 and 2006. Ranging in size and burn intensity, this subset of known fires offers an excellent sample from which to investigate the spectral and temporal effects which impact disturbance type classification. Here the fire perimeter data are used to guide the collection of sample data for training and validating the disturbance type map.

2.5. Forest disturbance type mapping

Forest disturbance maps were derived via multi-temporal RGB color composite analysis (Coppin et al., 2004; Sader & Winne, 1992;

Wilson & Sader, 2002). The basis of this approach relies on analyst interpretation of three dates of imagery which are simultaneously projected on the computer screen using the red, green, and blue color display channels. Using concepts from color additive theory, major changes in forest cover between image dates appear in unique combinations of primary and additive colors depending on which date of imagery is coupled with which RGB display channel. Although the RGB composite approach is based on interpretation of three dates of imagery at any one time, the spectral training signatures used to classify disturbance were derived using the full suite of images comprising the LTS. Thus, our application of RGB composite analysis is considered an analyst driven multi-temporal, multi-spectral change detection technique.

Here the RGB composite approach was used to collect training data through simultaneous interpretation of individual Landsat images, RGB color composites of B5, ancillary data (e.g., Google earth) and fire perimeters from the LFDB (Amiro et al., 2001; Stocks et al., 2003). We opted to interpret and classify B5 data, as the SWIR bands of Landsat have been previously found useful for characterizing both vegetation condition and for detecting forest disturbances (Cohen & Goward, 2004; Healey et al., 2006; Kennedy et al., 2007; Ranson et al., 2003). Passing the B5 image combinations through the RGB color gun we identified disturbance years, which were subsequently interpreted to be the result of fire or clearcutting through inspection of pre- and post-disturbance false color composite Landsat images and the LFDB perimeters (see Fig. 2 for an example). Using this guided change detection approach we iteratively located and identified fire and clearcut disturbances through time, from which we collected training samples for use in supervised classification. Training samples were collected to avoid interior undisturbed patches, while at the same time ensuring that the full range of spectral variability resulting from differences in topography, shadowing, and burn severity were captured. Collectively, the digitized training samples captured thousands of pixels per year and disturbance type. Although we mapped and validated disturbances occurring prior to the first image date (i.e., pre-1986), we excluded this disturbance interval from further analysis given the difficulty associated with knowing exactly when those disturbances took place on the landscape. Furthermore, spectral limitations prevented mapping fires which occurred in the last image date (i.e., 2008).

In addition to year and type of forest disturbance, we also classified persistent forest, persistent non-forest, and water classes. The term "persistent" is used to indicate that the forest or non-forest cover type stayed the same over the full 22 year period of observation. Here non-forest includes urban features, agricultural lands and other vegetated surfaces which were not determined to be forested (e.g., non-forested wetlands and bogs). To create the final disturbance map the collected training data and the stack of B5 images were used as inputs into a supervised minimum distance to means classifier (Jensen, 2004). Areas on the map which experienced multiple disturbances during the period of observation were coded so as to reflect the year of initial disturbance. After validating the accuracy of the disturbance map, the fires and clearcuts occurring between 1987 and 1995 were used to perform the iterative classification test described below in Section 2.7.

2.6. Disturbance map validation

The temporal depth of forest change information derived from LTS pose numerous challenges for collecting suitable reference data for map validation. Existing data sets can be difficult to retrieve and are often of insufficient temporal extent and resolution to adequately validate the possible annual time steps of satellite derived historical disturbance maps. Given that forest disturbances (at least those impacting the upper canopy) result in discrete spectral changes which can be reliably labeled by experienced analysts (Cohen et al., 1998; Masek et al., 2008), validation of LTS change maps has increasingly relied upon the use of interpreter labeled sampled

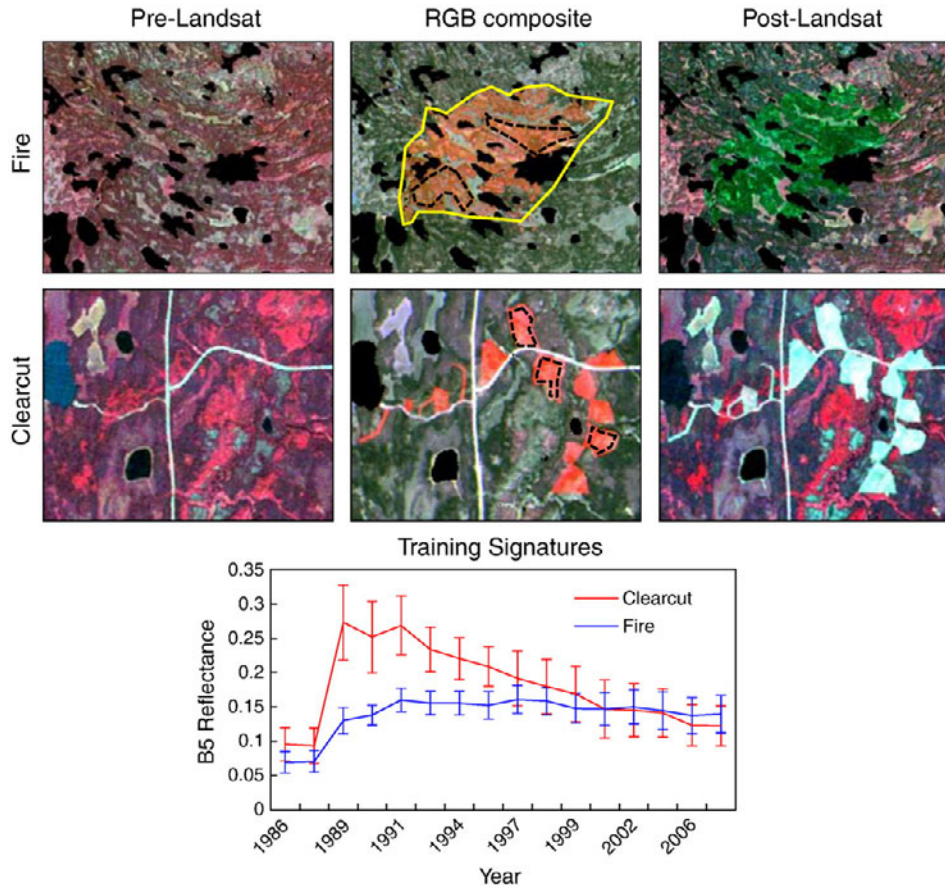


Fig. 2. An example of sample data collection using RGB composite change detection approach. RGB color composites of Landsat B5 were used to locate forest disturbances, which were interpreted as fire or clearcut using pre- and post-disturbance Landsat data (shown as 4,3,2 false color composite) and LFDB perimeters (yellow outline). Digitized samples (---) were used to develop training signatures for use in supervised classification.

points (e.g., Cohen et al., 2010; Thomas et al., 2011). Although high spatial resolution aerial photographs (e.g., Google earth images) and ancillary datasets such as national forest inventory data or GIS layers (e.g., LFDB) are often used to aid interpretation, in most cases the LTS images themselves serve as the primary data source from which reference data are collected. One benefit of this approach is that the entire landscape can be sampled and all years evaluated. In addition, the flexibility of this approach allows the use of any number of different design-based sampling schemes to calculate map accuracy.

Here we use a stratified random design where sample points are distributed according to strata, which are defined in this case by the individual disturbance map classes (both by year and type of disturbance). To account for the fact that the class area proportions are unbalanced we used inclusion probabilities to achieve design-based inference of map accuracy. For the samples in each stratum the inclusion probability, or probability that a particular map pixel is included in the sample, was calculated as: (# of pixels in strata/# of reference samples in

strata)/# of pixels in disturbance map (Stehman & Czaplewski, 1998). To achieve a reasonable balance between the number of samples required to fully validate the disturbance map and the time required for interpretation we elected to use a balanced sample of 30 points per class (there are 29 disturbance classes plus persistent forest, persistent non-forest, and water), resulting in a total of 960 validation sample points.

To minimize the error associated with co-locating single pixels, each validation sample consisted of a 3 × 3 pixel block, centered on the sample point location. A window majority rule was used which required at least 7 of the 9 pixels in the block to be of the same map class (Thomas et al., 2011). This allowed samples to be located close to class edges yet sufficiently distant that interpreter confusion was minimized. Reference data (i.e., year and type of disturbance) was collected for each sample point through simultaneous inspection of individual LTS images (displayed in chronological sequence from earliest to latest), B5 RGB color composites, high spatial resolution imagery (from Google earth) and plots of B5 spectral response

Table 2

The Landsat images used in the iterative classification test according to disturbance year and post-disturbance image interval.

Disturbance year	Post-disturbance image (time since disturbance)						
1987	1989 (2)	1990 (3)	1991 (4)	1993 (6)	1994 (7)	1995 (8)	1997 (10)
1989	1990 (1)	1991 (2)	1993 (4)	1994 (5)	1995 (6)	1997 (8)	1998 (9)
1990	1991 (1)	1993 (3)	1994 (4)	1995 (5)	1997 (7)	1998 (8)	1999 (9)
1991	1993 (2)	1994 (3)	1995 (4)	1997 (6)	1998 (7)	1999 (8)	2001 (10)
1993	1994 (1)	1995 (2)	1997 (4)	1998 (5)	1999 (6)	2001 (8)	2002 (9)
1994	1995 (1)	1997 (3)	1998 (4)	1999 (5)	2001 (7)	2002 (8)	2004 (10)
1995	1997 (2)	1998 (3)	1999 (4)	2001 (6)	2002 (7)	2004 (9)	2006 (11)

(similar in logic to the trajectory window in Cohen et al., 2010). The recorded reference data are used to generate an error matrix, as well as unbiased estimates of map accuracy.

2.7. Iterative classification test

To determine the impact that time since disturbance and spectral wavelength have on classification accuracy, we used the fire and clearcut disturbances mapped between 1987 and 1995 to perform an iterative classification test using the six Landsat bands/indices described in Section 2.3. Fire and clearcut patches larger than 15 ha (hectares) from these dates were buffered internally by 100 m to remove edge effects. For the remaining “core” fire and clearcut disturbance pixels, date-neutral time-since disturbance stacks were created, showing the sequence of bands/indices following the mapped disturbances. Because the Landsat images were not all acquired on an annual time step, the spectral data used in each post-disturbance image represented slightly different time intervals (Table 2). For labeling purposes we report time since disturbance as the amount of time which occurs most frequently in each post-disturbance image interval (see Table 2).

From these time-since disturbance stacks (one stack for each of the 6 tested bands or transformations), a random sample of spectral values from 500 burn pixels and 500 harvest pixels was assembled. For each band or index, 10 classifications were performed at each interval since disturbance (n=7, Table 2) to label disturbance cause at each of the core pixels. The “fire” and “harvest” classes were “trained” with a minimum distance to means classifier with 10 spectral values per disturbance type drawn randomly from the above pool of 500.

The remaining disturbance pixels not used for classification training were used to calculate Cohen’s kappa statistic (Jensen, 2004; Landis & Koch, 1977), a conservative measure of classification accuracy which accounts for chance agreement. A kappa of 1 is taken to represent perfect agreement and a kappa of 0 represents the level of agreement expected solely by random chance. The mean and standard deviation of the classification kappa values is reported for each of the Landsat bands/indices and time steps following disturbance. Additional descriptive statistics were collected relating spectral values for all core “fire” and

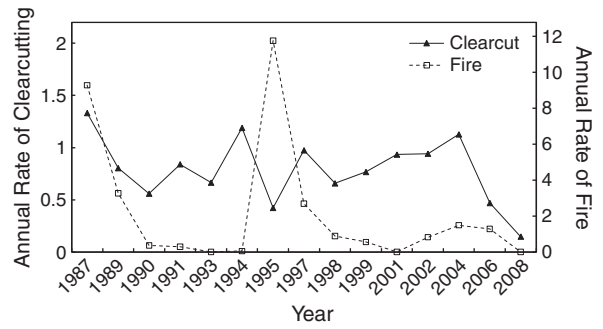


Fig. 4. Annual rate of forest disturbance, calculated as the percentage of total forest land disturbed in each year by fire and clearcutting.

“harvest” pixels at each time step to detail the stability and separability of signatures for the two disturbance processes under each of the six data types.

3. Results

3.1. Forest disturbance type map

Simultaneous interpretation of the individual Landsat images, B5 color composites, and the LFDB perimeters allowed for the successful identification and sampling of both wildfire and harvest disturbance types, as well as the persistent forest and non-forest classes. The combination of analyst-interpreted training data and the RGB color composite change detection approach yielded maps of both year and type of forest disturbance (Fig. 3a and b). Based on the disturbance map 3558 km² of forest area was disturbed in the study area during the 21 year period from 1987 to 2008 (21 years as disturbances mapped in first LTS image could not be temporally assigned). This amount of mapped disturbance equals 13.64% of the land base (excluding water and pre-1986 disturbance classes), of which 9.59% was attributed to fire and 4.05% to clearcutting.

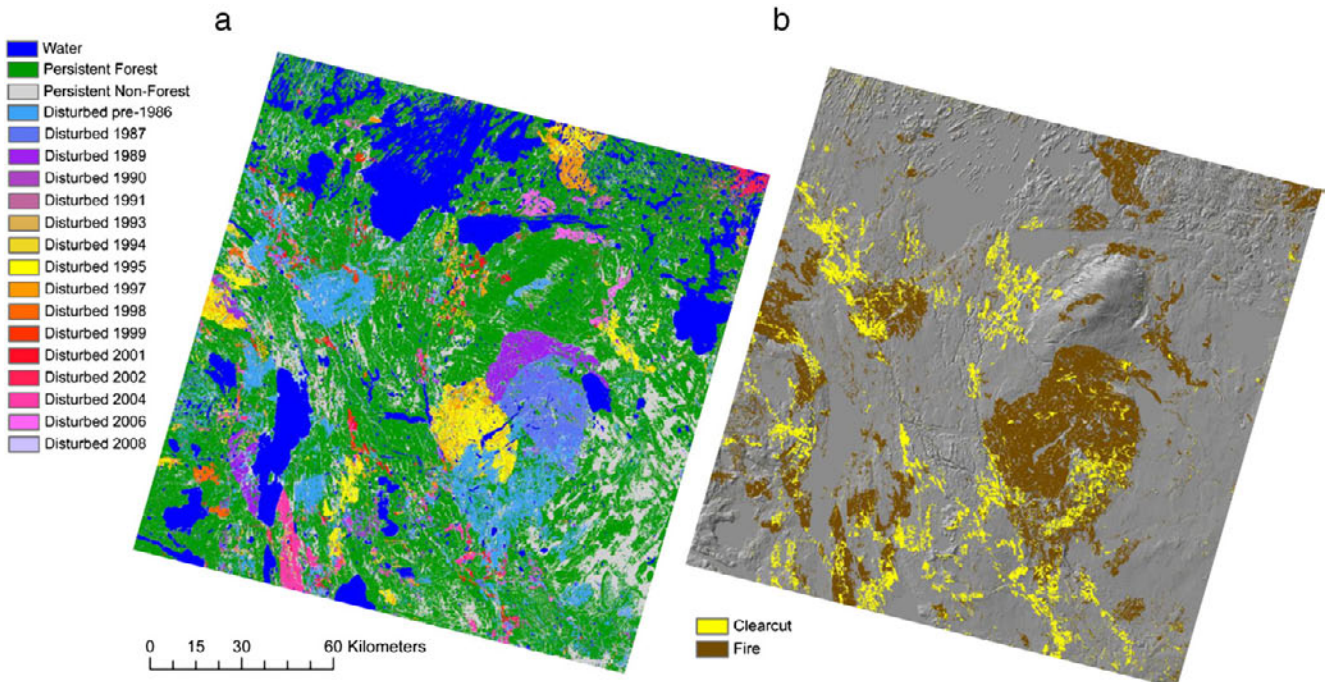


Fig. 3. Landsat disturbance maps showing year (a) and type (b) of forest disturbance.

The annual rate of forest disturbance was calculated by dividing the area mapped in each disturbance interval by the total area of forest disturbed between 1987 and 2008. Dividing this ratio by the number of years between each image acquisition resulted in the annual rate of forest disturbance (Fig. 4). As the spring 1986 and late summer 1987 images cover two summer harvesting periods we took this image pair to represent a two year interval when calculating annual rates. The results indicate that the annual rate of disturbance due to clearcutting stayed relatively consistent through time, with a maximum rate of disturbance (1.33%) in 1987 and a minimum (0.15%) in 2008. Annual rate of wildfire on the other hand were characterized by episodic fluctuations due to large fire years in 1987 (9.27%) and 1995 (11.74%), and no fires in 1993, 2001, and 2008. The average annual rate of forest disturbance in the study area over this 21 year period was 1.49% (2.18% from fire, 0.79% from clearcutting).

3.2. Disturbance type map validation

To validate the disturbance type map we compared it with the interpreted reference data using a standard error matrix. To achieve unbiased estimates the samples comprising the error matrix were weighted according to their inclusion probabilities as in Stehman and Czaplewski (1998). The weighted error matrix was used to calculate measures of overall agreement such as overall accuracy (calculated as the sum of values in the primary diagonal/total number of samples) and kappa, as well as per class user's and producer's accuracies. Commission and omission error were obtained by subtracting 100% from the user's and producer's accuracies respectively (Janssen & van der Wel, 1994).

Based on the error matrix shown in Table 3, the disturbance type map had an overall accuracy of 93%. The kappa value of 0.91 suggests a high level of agreement between the map and reference data, even after chance agreement is accounted for. When averaged over all map classes the user's accuracy and producer's accuracy indicate that the map has higher omission (7.5%) than commission (3.57%) error. The higher omission rate however is largely driven by the static classes (i.e., persistent forest, persistent non-forest, and water). When only the disturbance classes are considered, the map has higher overall commission error (7.93%). It should be noted that although the overall accuracy of the map was found to be high, the accuracy measures should be viewed with caution as the same interpreter was used to map disturbances and perform the validation. Although this bias potentially inflated the calculated accuracy metrics, the validation effort nevertheless provided an overall sense of map reliability, as well as highlighted the main sources of map error.

For instance, the majority of error in the disturbance map comes from the high omission error (27.11%) of the persistent non-forest class. This error is the result of known areas of persistent non-forest being incorrectly classified as disturbed (either by fire or clearcut) or persistent forest. These incorrectly classified areas are predominately non-forested wetlands, which can vary spectrally from year to year due to differences in precipitation, lake levels and the timing of bud break. These often sharp year to year phenological differences can result in spectral confusion with the forest disturbance classes.

The second most prevalent error in the disturbance map occurs when known areas of fire disturbance are incorrectly classified as clearcut. These map errors are the result of salvage harvesting which occurs shortly (i.e., the year or two) after a fire event, with precision in our case driven by the interval between image dates. In this instance the spectral response of fire disturbance is eclipsed by the stronger spectral change associated with clearcutting. In these situations the second, more spectrally discrete disturbance is captured by the classification algorithm. In situations where salvage harvesting occurs several years (or images) after a fire event, potential exists that more detailed training signatures could be developed to capture both disturbance types and inform upon forest salvage activities. Long term reporting of both harvest and burned area without compensating for

salvage will result in overestimation of disturbed area (essentially through double counting of the same locations).

A third type of error occurred when areas of fire were labeled with the wrong year of disturbance. This error occurred primarily in 1995 when areas of coniferous forest (which are spectrally dark in B5) were severely burned. The spectral similarity between pre-disturbance conifer forest and post-disturbance burn scar resulted in a two year (or one image interval) delay in detecting the onset of disturbance. While SWIR data alone were found to accurately classify year and type of disturbance, it is possible that including additional spectral bands and/or image transformations (e.g., multi-spectral classification) could help minimize these types of minor misclassification errors.

3.3. Iterative classification test

The kappa statistics derived via the iterative classification test revealed dramatic differences in the ability of the various Landsat spectral bands and vegetation indices to classify the fire and clearcut disturbances (Fig. 5). The results showed that all three Landsat bands/indices sensitive to forest structure effectively classified the disturbance types using imagery acquired 1 year after disturbance. Using this image, B5 recorded the highest overall kappa (0.89) of any of the six Landsat bands/indices tested. Although B5 scored the highest kappa, both wetness (kappa = 0.78) and FI (kappa = 0.81) also yielded high kappa scores. While B5 had the highest kappa when classifying the image acquired 1 year after disturbance, it still recorded a kappa of near perfect agreement (0.81) when classifying the image acquired 4 years after disturbance. Over time, the structure bands/indices all showed similar patterns of decreasing kappa. By 10 years after disturbance all three forest structure bands/indices yielded classifications that were no better than random chance. In addition to scoring the highest kappa, B5 displayed virtually no variation in kappa until 8 years after disturbance. Wetness displayed a consistently small amount of variation in each of the time since disturbance intervals. Although displaying a relatively small amount of variation early in time, FI displayed the highest variation (standard deviation = 0.19) of any of the structure bands/indices 8 years after disturbance.

Regardless of the amount of time after disturbance, the Landsat spectral indices primarily sensitive to green leaf area were not successful in classifying the disturbance types. Opposite of the structure data, the green leaf area indices all recorded their highest kappa scores when classifying the image acquired 10 years after disturbance (Fig. 5). The highest kappa was recorded by TCA (0.41), which at best could be interpreted only as moderate classification accuracy. All of the other kappa scores recorded by the green leaf area indices could be interpreted as having only fair to less than chance agreement. Over time, the green leaf indices all recorded similarly low patterns of kappa and relatively high levels of variation. Not only did NDVI display a relatively high level of variation through time, by year 10 after disturbance it had the highest overall variance (standard deviation = 0.38) of any of the six Landsat bands/indices tested. The maximum variance recorded by NDVI was twice as large as the maximum variance recorded by the structure bands/indices.

3.4. Spectral properties of core burned and harvested pixels

Descriptive analysis was made of the spectral values of the core fire and harvested pixels used in the iterative classification test. Fig. 6 shows the relationship among spectral values for burned, harvested and undisturbed forest pixels, as exhibited through each of the 6 studied bands or indices. Spectral values for fire and harvest are most separable from each other and from the general forest population in the SWIR-based bands: B5, Wetness and FI. Initial spectral differences between fire and harvests are also more durable over time in the SWIR bands than the bands influenced more directly by NIR reflectance.

Table 3
 Error matrix for the LTS disturbance type map. Class label abbreviations are: PF = persistent forest, PNF = persistent non-forest, CC = clearcut, F = fire. Numeric labels represent year of disturbance (e.g., 87 = 1987). Disturbances in 1986 represent areas that are not forested in time 1 but become forested by the last image date. Results are shown as area percentages (e.g., 40.43 refers to 40.43% of the LTS disturbance map). Note that the majority of samples fall along the primary diagonal of the matrix, indicating the map and reference data are in agreement. Off diagonal samples indicate errors, which in this case are mostly the result of fires which are incorrectly classified as clearcuts and persistent non-forest areas which are incorrectly classified as forest disturbance.

LTS map	Reference data																								Total	n	Users									
	PF	PNF	Water	86 CC	87 CC	89 CC	90 CC	91 CC	93 CC	94 CC	95 CC	97 CC	98 CC	99 CC	01 CC	02 CC	04 CC	06 CC	08 CC	86 F	87 F	89 F	90 F	91 F				94 F	95 F	97 F	98 F	99 F	02 F	04 F	06 F	
PF	40.43	4.49																																44.93	30	90.00
PNF		15.61																																15.61	30	100.00
Water			15.89																															15.89	30	100.00
86 CC			0.08	2.16																0.16														2.40	30	90.00
87 CC			0.13		0.81																													0.94	30	86.67
89 CC			0.02			0.40																0.02	0.09											0.52	30	76.67
90 CC							0.13																											0.13	30	100.00
91 CC								0.33																										0.33	30	100.00
93 CC									0.31	0.01	0.01																							0.33	30	93.33
94 CC										0.33	0.01												0.01											0.35	30	93.33
95 CC											0.07																							0.07	30	100.00
97 CC												0.36																						0.46	30	76.67
98 CC													0.38														0.11							0.66	30	56.67
99 CC														0.13																				0.13	30	100.00
01 CC															0.34																			0.36	30	93.33
02 CC																0.27																		0.27	30	100.00
04 CC																	0.39																	0.40	30	96.67
06 CC																		0.16																0.16	30	100.00
08 CC																			0.06															0.16	30	100.00
86 F																					0.06													0.07	30	86.67
87 F																						5.23												5.81	30	90.00
89 F																							1.86											1.93	30	96.67
90 F																							1.18											1.18	30	100.00
91 F																							0.01	0.06										0.07	30	90.00
94 F																									0.08									0.08	30	100.00
95 F																										0.03								0.03	30	100.00
97 F																											2.27							2.27	30	100.00
98 F																											0.39	1.08						1.47	30	73.33
99 F																																		0.19	30	100.00
02 F																																		0.17	30	90.00
04 F																																		1.12	30	93.33
06 F																																		0.64	30	93.33
Total	40.46	21.41	15.89	2.16	0.81	0.40	0.13	0.33	0.31	0.34	0.09	0.36	0.38	0.13	0.34	0.27	0.39	0.21	0.06	5.38	1.88	1.29	0.06	0.08	0.03	2.77	1.08	0.19	0.16	1.12	0.64	0.85	100.00	960		
n	28	63	30	28	26	23	30	31	28	29	32	23	17	30	28	30	29	32	26	29	30	39	27	29	30	45	22	30	28	28	28	32			Overall	0.93
Producers	99.94	72.89	100.00	99.74	100.00	100.00	100.00	100.00	100.00	96.76	76.00	100.00	100.00	100.00	100.00	100.00	100.00	79.07	100.00	97.03	99.08	91.81	100.00	100.00	100.00	81.92	100.00	100.00	92.60	100.00	100.00	98.97			Kappa	0.91

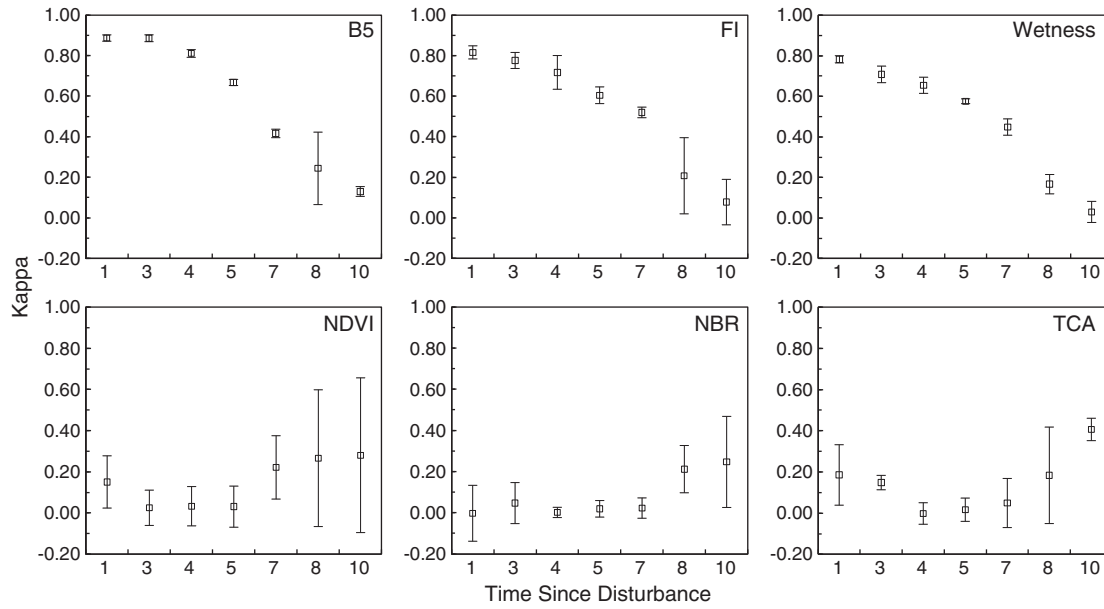


Fig. 5. Average kappa for the six Landsat spectral bands/indices based on 10 iterative classifications per time since disturbance interval. Error bars represent ± 1 standard deviations.

4. Discussion

4.1. Forest disturbance type mapping

In this study, an analyst driven RGB color composite change detection approach was used to map year and type of forest disturbance through time using a 22 year (16 image) LTS. Others have found RGB composite analysis to be a useful method for mapping changes in forest cover over time (Hayes & Sader, 2001; Healey et al., 2005; Wilson & Sader, 2002) and here we extended the application to map patterns of spectral change associated with fire and clearcut disturbance events. The simultaneous interpretation of LFDB burn perimeters, individual Landsat images and RGB color composites provided the necessary backdrop for mapping both the timing and cause of forest disturbance. By using the full temporal context of the multi-temporal Landsat data, we found that within the general signal

of forest disturbance each of the disturbance types yielded distinctly different patterns of SWIR reflectance (e.g., see B5 Fig. 2), allowing their successful classification through space and time.

The disturbance type map was found to have high overall accuracy (93%) even after accounting for chance agreement (i.e., kappa = 0.91). Aside from minor misclassifications which resulted from image misregistration and cloud filtering, the majority of map error was the result of persistent non-forest (in particular bogs and wetlands) being misclassified as forest disturbance and areas burned by fire being misclassified as clearcut.

Eliminating false change detections that occur in wetland areas is extremely difficult when using imagery acquired on an annual time step. Wetlands are a land condition, not exclusively cover, and are subject to intra- and inter-annual variations based upon considerations including water levels, precipitation amounts and weather. Natural fluctuations in the timing of bud break and lake water levels

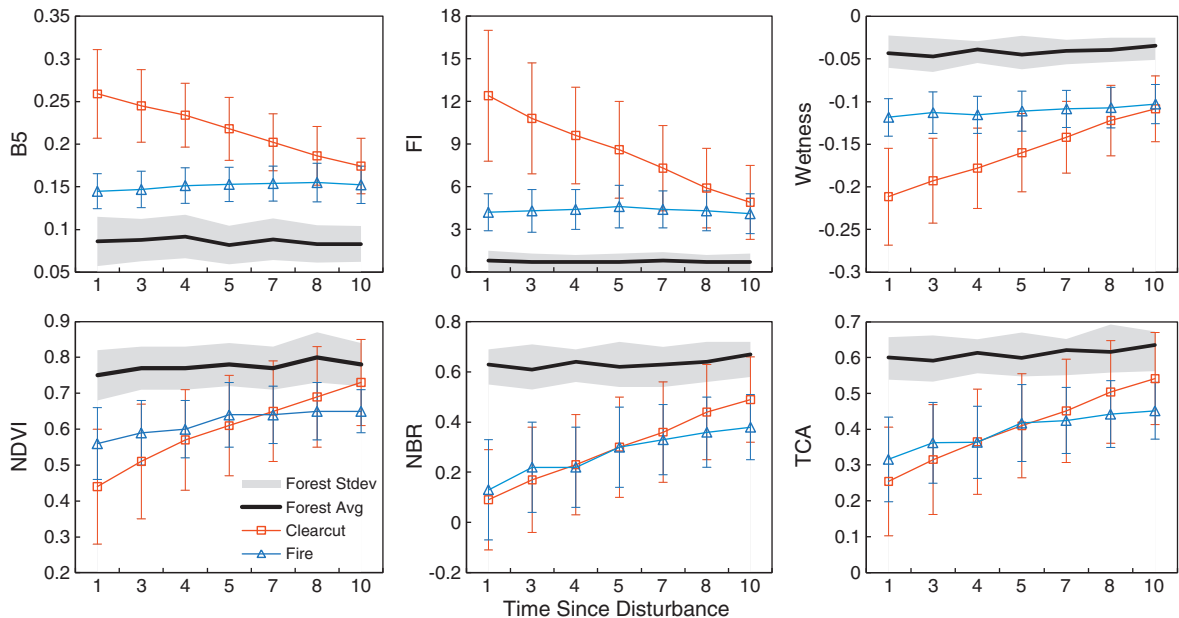


Fig. 6. Average spectral response of the six Landsat bands/indices to fire and clearcutting according to time since disturbance. Error bars represent ± 1 standard deviations.

can result in large, year to year spectral changes which resemble the discrete spectral change typically associated with forest disturbance. Furthermore, the annual image time step (i.e., 1 image date per growing season) makes it extremely difficult to detect non-stand replacing disturbances (e.g., fire or thinning) which occur immediately prior to stand replacing disturbances (e.g., clearcut salvage harvesting). It is interesting to note that both main types of error (wetland misclassification and omission of non-stand replacing disturbance) observed in this study have been previously found to occur in other LTS change maps derived on an annual time step (Huang et al., 2010a; Thomas et al., 2011).

Improving LTS temporal precision through the use of intra-annual images could help minimize false change detections which occur in wetland areas and could also lead to better disturbance type attribution in areas which undergo multiple disturbances. Lastly, increased LTS temporal precision would also stand to improve the performance of cloud filtering algorithms, thus minimizing misclassifications which can occur when disturbances fall within filtered areas. Aside from identifying potential improvements, our validation confirms that the disturbance type map is of high overall quality and is thus suitable for exploring the spectral and temporal properties of clearcut and fire disturbances.

4.2. Spectral properties of fire and clearcut disturbance types

The classification test showed that the three SWIR-based Landsat bands/indices associated with forest structure, shadowing, and canopy moisture content were most effective at discriminating the fire and clearcut disturbance types. Clearcutting involves removing most of the forest canopy on a site, thus it resulted in a large initial change in spectral values (Fig. 6). Depending on burn severity, fires remove variable amounts of forest canopy cover, leaving behind a complex mosaic of live vegetation, downed wood and dead standing trees. This complex mosaic of ground cover results in more shadowing and structure, which provides for less spectral change than caused by the clearcut disturbances (Fig. 6). Ultimately it was this initial difference in magnitude of spectral change which led to the accurate separation of the two disturbance types. Although Landsat B5 achieved the highest overall kappa (Fig. 5) we believe all the SWIR-based bands/indices have the potential to accurately classify the two disturbance types, especially when imagery is acquired on an annual or biannual (e.g., 1 to 2 years after disturbance) time step. Given the additional processing and storage costs of the transformations, though, B5 alone is likely to be suitable for many applications.

The structural differences associated with the loss of forest canopy cover persisted for several years such that the disturbance types were still accurately classified (e.g., $\text{kappa} \geq 0.80$) up to 4 years after disturbance. This is an important finding as many areas in northern boreal forests are impacted by frequent cloud and snow cover, limiting the number of clear images from which to map forest change with Landsat data. In cases where imagery is not available it is promising that accurate disturbance type classification can still be achieved within this slightly longer acquisition window. As time progressed and successional recovery of vegetation began to dominate the spectral signal, the fire and clearcut disturbances began to overlap in spectral space (Fig. 6), causing kappa to steadily decline after about 5 years post-disturbance (Fig. 5). By 8 to 10 years after disturbance the kappa scores indicated that classification was no better than random agreement. The diminishing detectability of fire disturbance over time found here is supported by similar findings in research on the capture of insect infestation (Wulder et al., 2005).

The green leaf area indices on the other hand, all achieved unreliably low kappa scores (Fig. 5), indicating that they could not distinguish wildfires and clearcut harvests regardless of time since disturbance. The spectral data show that the green leaf indices all responded similarly to the loss of forest canopy cover initiated by fire

and clearcut disturbance (Fig. 6). Although clearcuts seemed to produce a slightly larger loss of leaf area, the relatively similar magnitude of spectral change the year after disturbance suggests that there was either very little difference in the amount of vegetation/canopy cover initially removed by the two disturbance agents, or that the vegetation indices did not consistently respond to the physical differences brought on by fire and clearcutting. While it is beyond the scope of this study to infer which of these factors is driving the initial response of green leaf area, it is worth noting that others have found that changes in near-infrared reflectance (used in part to develop NDVI and NBR) do not always correlate well with disturbance events (Healey et al., 2006; Huang et al., 2010a; Olsson, 1994). The potentially unpredictable response of near-infrared reflectance to disturbance may also be a factor in some questioning the consistency of NBR response to various levels of burn severity (French et al., 2008; Roy et al., 2006; Wulder et al., 2009b).

In contrast to the structure data, the green leaf area indices all recorded their highest kappa scores when classifying the image acquired 10 years after disturbance (Fig. 5). This rise in accuracy is due to the steeper slope of leaf area recovery for clearcuts, which by 8 to 10 years after disturbance resulted in a noticeable degree of spectral separation from fires (Fig. 6). Although average kappa scores increased over time, so too did the variance (Fig. 5), indicating that the recovery of green leaf area is highly variable for both fire and clearcut disturbances. This spectral variability meant that the classification results were more heavily impacted by the random selection of training pixels used in the iterative classification test. Though the spectral overlap prevented discrimination of the two disturbances, it is interesting to note that on average clearcuts seem to recover green leaf area more quickly than fires (Fig. 6).

We foresee that the results of this study could support amendment of current change detection algorithms to carry out automated labeling of cause of disturbance in the boreal forests of Canada. Additional decision rules based on identified FI thresholds could be added to VCT (Huang et al., 2010a), for example, while the differential trajectories shown in Fig. 6 could be used in a trend-based algorithm such as LandTrendr (Kennedy et al., 2010) to estimate disturbance causes. This type of investigation is envisioned to provide a template in support of developing broader application of semi-empirical, automated approaches to attributing causal agents to mapped disturbances.

4.3. Applications of disturbance type maps

The disturbance type map indicates that 13.64% of the forested land base was disturbed in the study area between 1987 and 2008. While high levels of disturbance such as observed here are relatively common in boreal forests, studies have shown that disturbance from fire and clearcut harvesting impact forest composition (Johnstone et al., 2004; McRae et al., 2001), forest fragmentation (Fitzsimmons, 2003), biodiversity (Bradshaw et al., 2009; Peltzer et al., 2000), bird habitat (Hobson & Schieck, 1999), and water quality (Pinel-Alloul et al., 2002) in different ways. Thus, maps which attribute cause of disturbance offer several advantages over maps which simply label timing of disturbance. We briefly present three examples showcasing potential applications of disturbance type maps.

4.3.1. Policy and management

Once disturbance types are partitioned it is evident that the primary disturbance agent in the study area is large fire events. Whereas fire events episodically disturbed large areas, clearcutting affected less area but was more consistent through time. The classification results showed that the level of clearcutting within the study area dropped to its lowest rate (0.15%) in 21 years in 2008. North American forest harvest rates are typically correlated with forest product markets (Masek et al., in press), thus U.S. housing starts are often used as a surrogate for timber and pulp demand in Canada. As U.S. housing starts also reached their lowest levels

in more than five decades in 2008 (U.S. Census Bureau, 2010¹) it is possible that the weakened global and U.S. economic conditions beginning in 2006 resulted in a slowing of harvesting activities in Canada (Natural Resources Canada, 2010²) that may have been evidenced in the study area. We recognize that as time progresses harvesting over any given managed forest must decrease as the previously harvested areas become ineligible for re-harvesting given the period of time necessary for suitable regeneration to occur. Wildfire in areas that could have otherwise been eligible for harvesting further serve to reduce the rate of forest clearing in statically defined study regions. Nonetheless, as our change map resolves both year and type of disturbance, subtle changes in harvesting levels can be more easily ascribed to the economic, social and environmental policies which might be influencing their temporal patterns.

Opportunities exist with the approach demonstrated to produce meaningful associations between policy/management and disturbance rates when the findings are considered in the context of a particular management (say a timber supply area) or ecologically meaningful spatial unit (e.g., watershed and ecozone). In some cases, more contextually meaningful study areas will require extending the RGB change detection approach to larger spatial extents. Although our application of the RGB change detection approach did require significant expertise in image interpretation, it is possible that the temporal signatures developed with our user intensive approach could be extended to larger areas through incorporation with automated disturbance mapping algorithms.

4.3.2. Estimating burned area

Burned area is an important variable required to estimate carbon emissions from wildfire. Although the LFDB is an excellent source of information regarding the timing and location of Canadian wildfires, the burn perimeters are digitized by a number of different agencies and interpreters; thus, accuracy can be of variable quality. Although more recent records in the LFDB are from satellite-based observations, it has been shown that manually interpreted fire perimeters and coarse resolution satellite classifications tend to overestimate burned area (Fraser et al., 2004) due to inclusion of unburned islands and other non-forest land features (e.g., water). Disturbance type maps, such as the one produced here, offer a potentially more reliable way of estimating burned area as the spatial resolution of Landsat allows for the exclusion of unburned areas (and other non-forested land features such as water), as well as detection of smaller fires (<200 ha) which are not included in the LFDB. Given disparities in data quality, scale and accuracy it is not surprising that the LFDB perimeters and LTS disturbance map result in different year-to-year estimates of burned area. As these differences can be especially pronounced in large fire years (e.g., we found a 35% difference between mapped burned area and LFDB burned area in 1987 and a 51% difference in 1995) it is possible that previous studies which used LFDB perimeters to estimate carbon emissions overestimated the amount of land area affected by fire. Amiro et al. (2001), for example, assume that unburned islands make up less than 5% of the area within burn perimeters. The results of our study suggest that LTS-based maps which accurately separate fire from other disturbances may offer new insight into burn area heterogeneity occurring within burn boundaries, as well as refined estimation of the amount of land area affected by fire.

4.3.3. Tracking vegetation recovery

Given the link between green leaf area and the photosynthetic capacity of vegetation, tracking forest recovery through monitoring of spectral data such as NDVI has important implications for estimating productivity (e.g., NPP) of forests. At the pixel level spectral recovery is impacted by the severity of disturbance and the rate and composition of

regrowing vegetation. When viewed with coarse spatial resolution imagery vegetation dynamics can spectrally mix with unburned islands and other non-forested land features, resulting in potentially accelerated recovery signals. For example, studies which have tracked post-fire NDVI recovery in boreal forests have found spectral recovery times to be 6 (Goetz et al., 2006) to 9 years (Hicke et al., 2003) when using 8-km Advanced Very High Resolution Radiometer (AVHRR) imagery and 15 years when using 1 km MODIS imagery (Cuevas-González et al., 2009). Our 30 m data suggest that NDVI in severely burned areas could take upwards of 20 years to fully recover to pre-fire levels. This demonstrates how scaling and spectral mixing can influence the calculated rate of spectral recovery (i.e., larger pixels = faster recovery times). Although the ecological relationship between spectral recovery and forest regeneration is not well understood, the use of Landsat disturbance type maps such as the one produced in this study should help minimize unwanted spectral mixing, allowing for at minimum a better characterization of areas which are progressing toward successful tree re-establishment versus those areas which may have become stagnated in earlier stages of succession.

5. Conclusion

In this study we used an RGB composite change detection approach to interpret and train a supervised classification in which fire and clearcut harvest disturbances were accurately mapped through time using a dense time series of B5 data from Landsat. Using the disturbance map we performed a classification test which demonstrated that spectral data from the SWIR (e.g., B5, Wetness and FI)) portion of the electromagnetic spectrum was most effective at separating fires and clearcut harvests possibly due to differences in structure, shadowing, and amounts of exposed soil left behind by the two disturbance types. Although B5 data acquired 1 year after disturbance produced the most accurate classification of the disturbance types, good separation could still be achieved up to 4 years after disturbance. The classification test also showed that fire and clearcut disturbances initiated similar patterns of initial loss and accrual of green leaf area which prevented successful disturbance type classification with vegetation indices such as NDVI. Several potential uses of LTS disturbance type maps were discussed, such as linking social and economic policy to harvesting rates, estimating burned area and tracking rates of post-disturbance vegetation recovery. Overall, given the distinct temporal response of SWIR reflectance produced by fire and clearcut harvests, we are encouraged that, following additional research, automated disturbance type mapping may be increasingly feasible. Expanding currently applied LTS algorithms – which are capable of mapping timing, extent, and magnitude of forest disturbance – to also include disturbance type would be a significant development. As disturbance from fire and harvesting have vastly different carbon consequences, improving capacity to accurately attribute disturbance type through space and time stands to benefit future studies aimed at quantifying the environmental impacts associated with forest disturbance in Canadian boreal forests and elsewhere.

Acknowledgments

This research was funded by the National Aeronautics and Space Administration (NASA) Terrestrial Ecosystems Program through the North American Forest Dynamics Project. Additional support was provided by the Interior West Region of the Forest Service's Forest Inventory and Analysis (FIA) Program. Technical assistance was provided by Nancy Thomas, Chenquan Huang, and Sam Goward of the University of Maryland. Landsat image processing from the LEDAPS system was graciously provided by Jeffrey Masek of NASA. The Government Related Initiatives Program (GRIP) of the Canadian Space Agency is acknowledged for supporting a portion of the involvement of Wulder in this research. Lastly, the insightful

¹ http://www.data360.org/dsg.aspx?Data_Set_Group_Id=47.

² <http://canadaforests.nrcan.gc.ca/statsprofile>.

alteration of the Landsat data policy of the United States Geological Survey (USGS) is acknowledged and appreciated for making this and similar endeavors possible.

References

- Amiro, B. D., Todd, J. B., Wotton, B. M., Logan, K. A., Flannigan, M. D., Stocks, B. J., Mason, J. A., Martell, D. L., & Hirsch, K. G. (2001). Direct carbon emissions from Canadian forest fires, 1959–1999. *Canadian Journal of Forest Research*, 31, 512–525.
- Asrar, G., Fuchs, M., Kanemasu, E. T., & Hatfield, J. L. (1984). Estimating absorbed photosynthetic radiation and leaf area index from spectral reflectance in wheat. *Agronomy Journal*, 76, 300–306.
- Baret, F., & Guyot, G. (1991). Potentials and limits of vegetation indices for LAI and APAR assessment. *Remote Sensing of Environment*, 35, 161–173.
- Birdsey, R. A., Jenkins, J. C., Johnston, M., Huber-Sannwald, E., Amiro, B., de Jong, B., Barra, J. D. E., French, N., Garcia-Oliva, F., Harmon, M., Heath, L. S., Jaramillo, V. J., Johnsen, K., Law, B. E., Marin-Spiotta, E., Maser, O., Neilson, R., Pan, Y., & Pregitzer, K. S. (2007). North American forests. In A. W. King, L. Dilling, G. P. Zimmerman, D. M. Fairman, R. A. Houghton, G. Marland, A. Z. Rose, & T. J. Wilbanks (Eds.), *The First State of the Carbon Cycle Report (SOCCR): The North American carbon budget and implications for the global carbon cycle* (pp. 117–126). Asheville, NC: National Oceanic and Atmospheric Administration, National Climatic Data Center.
- Bradshaw, C. J. A., Warkentin, I. G., & Sodhi, N. S. (2009). Urgent preservation of boreal carbon stocks and biodiversity. *Trends in Ecology & Evolution*, 24, 541–548.
- Brandt, J. (2009). The extent of the North American boreal zone. *Environmental Reviews*, 17, 101–161.
- Canty, M. J., & Nielsen, A. A. (2008). Automatic radiometric normalization of multitemporal satellite imagery with the iteratively re-weighted MAD transformation. *Remote Sensing of Environment*, 112, 1025–1036.
- Cohen, W. B., & Spies, T. A. (1992). Estimating structural attributes of Douglas-fir/western hemlock forest stands from Landsat and SPOT imagery. *Remote Sensing of Environment*, 41, 1–17.
- Cohen, W. B., Fiorella, M., Gray, J., Helmer, E., & Anderson, K. (1998). An efficient and accurate method for mapping forest clearcuts in the Pacific Northwest using Landsat imagery. *Photogrammetric Engineering and Remote Sensing*, 64, 293–300.
- Cohen, W. B., Maersperger, T. K., Gower, S. T., & Turner, D. P. (2003). An improved strategy for regression of biophysical variables and Landsat ETM+ data. *Remote Sensing of Environment*, 84, 561–571.
- Cohen, W. B., & Goward, S. N. (2004). Landsat's role in ecological applications of remote sensing. *Bioscience*, 54, 535–545.
- Cohen, W. B., Yang, Z., & Kennedy, R. (2010). Detecting trends in forest disturbance and recovery using yearly Landsat time series: 2. TimeSync – Tools for calibration and validation. *Remote Sensing of Environment*, 114, 2911–2924.
- Coops, N. C., Wulder, M. A., & Iwanicka, D. (2009). Large area monitoring with a MODIS-based Disturbance Index (DI) sensitive to annual seasonal variations. *Remote Sensing of Environment*, 113, 1250–1261.
- Coppin, P., Jonckheere, I., Nackaerts, K., Muys, B., & Lambin, E. (2004). Digital change detection methods in ecosystem monitoring: A review. *International Journal of Remote Sensing*, 25, 1565–1596.
- Crist, E. P., & Cicone, R. C. (1984). A physically-based transformation of Thematic Mapper data – The TM tasseled cap. *IEEE Transactions on Geoscience and Remote Sensing*, GE, 22, 256–263.
- Crist, E. P. (1985). A TM tasseled cap equivalent transformation for reflectance factor data. *Remote Sensing of Environment*, 17, 301–306.
- Cuevas-González, M., Gerard, F., Balzter, H., & Riaño, D. (2009). Analysing forest recovery after wildfire disturbance in boreal Siberia using remotely sensed vegetation indices. *Global Change Biology*, 15, 561–577.
- Easterling, D. R., Karl, T. R., Gallo, K. P., Robinson, D. A., Trenberth, K. E., & Dai, A. (2000). Observed climate variability and change of relevance to the biosphere. *Journal of Geophysical Research*, 105(D15), 20101–20114.
- Eidenshink, J., Schwind, B., Brewer, K., Zhu, Z. L., Quayle, B., & Howard, S. (2007). A project for monitoring trends in burn severity. *Fire Ecology Special Issue*, 3, 3–21.
- Elvidge, C. D. (1990). Visible and near infrared reflectance characteristics of dry plant materials. *International Journal of Remote Sensing*, 11, 1775–1795.
- Fitzsimmons, M. (2003). Effects of deforestation and reforestation on landscape spatial structure in boreal Saskatchewan, Canada. *Forest Ecology and Management*, 174, 577–592.
- Fraser, R. H., Hall, R. J., Landry, R., Lynham, T. J., Lee, B. S., & Li, Z. (2004). Validation and calibration of Canada-wide coarse-resolution satellite burned area maps. *Photogrammetric Engineering and Remote Sensing*, 70, 451–460.
- French, N. H., Kasischke, E. S., Hall, R. J., Murphy, K. A., Verbyla, D. L., Hoy, E. E., & Allen, J. L. (2008). Using Landsat data to assess fire and burn severity in the North American boreal forest region: An overview and summary of results. *International Journal of Wildland Fire*, 17, 443–462.
- Fricker, J. M., Chen, H. Y. H., & Wang, J. R. (2006). Stand age structural dynamics of North American boreal forests and implications for forest management. *International Forestry Review*, 8, 395–405.
- Giglio, L., Loboda, T., Roy, D. P., Quayle, B., & Justice, C. O. (2009). An active-fire based burned area mapping algorithm for the MODIS sensor. *Remote Sensing of Environment*, 113, 408–420.
- Gillett, N. P., Weaver, A. J., Zwiers, F. W., & Flannigan, M. D. (2004). Detecting the effect of climate change on Canadian forest fires. *Geophysical Research Letters*, 31, L18211.
- Gluck, M. J., & Rempel, R. S. (1996). Structural characteristics of post-wildfire and clearcut landscapes. *Environmental Monitoring and Assessment*, 39, 435–450.
- Goetz, S. J., Fiske, G. J., & Bunn, A. G. (2006). Using satellite time series data sets to analyze fire disturbance and forest recovery across Canada. *Remote Sensing of Environment*, 101, 352–365.
- Goetz, S. J., Baccini, A., Laporte, N., Johns, T., Walker, W., Kellendorfer, J., Houghton, R. A., & Sun, M. (2009). Mapping and monitoring carbon stocks with satellite observations: A comparison of methods. *Carbon Balance and Management*, 4, 2, doi:10.1186/1750-0680-4-2.
- Government of Canada (1995). *Sustaining Canada's forests: Timber harvesting*. SOE Bulletin No. 95–4. Ottawa, ON: Environment Canada.
- Government of Canada (1996). *The state of Canada's environment – 1996* (pp. 10–40). Ottawa, ON: Environment Canada.
- Government of Canada (2008). *National Forestry Database Program*. Ottawa, ON: Canadian Council of Forest Ministers Available at: http://nfdp.cfm.org/index_e.php.
- Harmon, M. E. (2001). Carbon sequestration in forests: Addressing the scale question. *Journal of Forestry*, 4, 24–29.
- Hayes, D. J., & Sader, S. A. (2001). Comparison of change-detection techniques for monitoring tropical forest clearing and vegetation regrowth in a time series. *Photogrammetric Engineering and Remote Sensing*, 67, 1067–1075.
- Healey, S. P., Cohen, W. B., Zhiqiang, Y., & Krankina, O. N. (2005). Comparison of tasseled cap-based Landsat data structures for use in forest disturbance detection. *Remote Sensing of Environment*, 97, 301–310.
- Healey, S. P., Yang, Z., Cohen, W. B., & Pierce, D. J. (2006). Application of two regression-based methods to estimate the effects of partial harvest on forest structure using Landsat data. *Remote Sensing of Environment*, 101, 115–126.
- Healey, S. P., Cohen, W. B., Spies, T. A., Moeur, M., Pflugmacher, D., Whitley, M. G., & Lefsky, M. (2008). The relative impact of harvest and fire upon landscape-level dynamics of older forests: Lessons from the Northwest Forest Plan. *Ecosystems*, 11, 1106–1119.
- Heinselman, H. L. (1983). Fire and succession in the conifer forests of northern North America. In D. C. West, H. H. Shugart, & D. B. Botkin (Eds.), *Forest succession, concepts and application* (pp. 374–405). New York, NY: Springer-Verlag.
- Hicke, J. A., Asner, G. P., Kasischke, E. S., French, N. H. F., Randerson, J. T., Collatz, G. J., et al. (2003). Postfire response of North American boreal forest net primary productivity analyzed with satellite observations. *Global Change Biology*, 9, 1145–1157.
- Hobson, K. A., & Schieck, J. (1999). Changes in bird communities in boreal mixedwood forest: Harvest and wildfire effects over 30 years. *Ecological Applications*, 9, 849–863.
- Huang, C., Song, K., Kim, S., Townshend, J. R. G., Davis, P., Masek, J. G., & Goward, S. N. (2008). Use of a dark object concept and support vector machines to automate forest cover change analysis. *Remote Sensing of Environment*, 112, 970–985.
- Huang, C., Goward, S. N., Masek, J. G., Gao, F., Vermote, E. F., Thomas, N., Schleeweis, K., Kennedy, R. E., Zhu, Z., Eidenshink, J. C., & Townshend, J. R. G. (2009). Development of time series stacks of Landsat images for reconstructing forest disturbance history. *International Journal of Digital Earth*, 2, 195–218.
- Huang, C., Goward, S. N., Masek, J. G., Thomas, N., Zhu, Z., & Vogelmann, J. E. (2010a). An automated approach for reconstructing recent forest disturbance history using dense Landsat time series stacks. *Remote Sensing of Environment*, 114, 183–198.
- Huang, C., Thomas, N., Goward, S. N., Masek, J. G., Zhu, Z., Townshend, J. R. G., & Vogelmann, J. E. (2010b). Automated masking of cloud and cloud shadow for forest change analysis. *International Journal of Remote Sensing*, 31, 5449–5464.
- Horler, D. N. H., & Ahern, F. J. (1986). Forestry information content of Thematic Mapper data. *International Journal of Remote Sensing*, 7, 405–428.
- Huete, A. R. (1988). A soil-adjusted vegetation index (SAVI). *Remote Sensing of Environment*, 25, 295–309.
- Ilisson, T., & Chen, H. Y. H. (2009). Response of six boreal tree species to stand replacing fire and cutting. *Ecosystems*, 12, 820–829.
- Janssen, L. L. F., & van der Wel, F. J. M. (1994). Accuracy assessment of satellite derived land-cover data: A review. *Photogrammetric Engineering and Remote Sensing*, 67, 1067–1075.
- Jensen, J. R. (2004). *Introductory digital image processing* (Third Edition). Upper Saddle River, NJ: Prentice-Hall 544 pp.
- Johnstone, J. F., Chapin, F. S., III, Foote, J., Kemmett, S., Price, K., & Viereck, L. (2004). Decadal observations of tree regeneration following fire in boreal forests. *Canadian Journal of Forest Research*, 34, 267–273.
- Kasischke, E. S., & Turetsky, M. R. (2006). Recent changes in the fire regime across the North American boreal region – Spatial and temporal patterns of burning across Canada and Alaska. *Geophysical Research Letters*, 33, L09703.
- Kennedy, R. E., Cohen, W. B., & Schroeder, T. A. (2007). Trajectory-based change detection for automated characterization of forest disturbance dynamics. *Remote Sensing of Environment*, 110, 370–386.
- Kennedy, R. E., Yang, Z., & Cohen, W. B. (2010). Detecting trends in forest disturbance and recovery using yearly Landsat time series: 1. LandTrendr – Temporal segmentation algorithms. *Remote Sensing of Environment*, 114, 2897–2910.
- Key, C. H., & Benson, N. C. (2005). Landscape assessment: Remote sensing of severity, the Normalized Burn Ratio. *FIREMON: Fire effects monitoring and inventory system*. In D. C. Lutes (Ed.), *USDA Forest Service General Technical Report RMRS-GTR-164-CD*. Ogden, UT. (pp. LA1–LA51).
- Key, C. H. (2006). Ecological and sampling constraints on defining landscape fire severity. *Fire Ecology*, 2, 234–259.
- Kurz, W. A., & Apps, M. J. (1999). A 70-year retrospective analysis of carbon fluxes in the Canadian forest sector. *Ecological Applications*, 9, 526–547.
- Kurz, W. A., Dymond, C. C., White, T. M., Stinson, G., Shaw, C. H., Rampley, G. J., Smyth, C., Simpson, B. N., Neilson, E. T., Trofymow, J. A., Metsaranta, J., & Apps, M. J. (2009). CBM-CFS3: A model of carbon-dynamics in forestry and land-use change implementing IPCC standards. *Ecological Modelling*, 220, 480–504.

- Lands Directorate (1986). *Terrestrial ecozones of Canada. Ecological land classification No. 19* 26 pp.
- Landis, J. R., & Koch, G. G. (1977). The measurement of observer agreement for categorical data. *Biometrics*, 33, 159–174.
- Larsson, H. (1993). Linear regression for canopy cover estimation in Acacia woodlands using Landsat-TM, -MSS, and SPOT HRV XS data. *International Journal of Remote Sensing*, 14, 2129–2136.
- Marshall, I. B., & Schut, P. H. (1999). A national ecological framework for Canada – Overview. *Ecosystems Science Directorate – Environment Canada, Research Branch – Agriculture and Agri-Food Canada, Ottawa, ON* 9 pp.
- Masek, J. G., Vermote, E. F., Saleous, N. E., Wolfe, R., Hall, F. G., Huemmrich, K. F., Feng, G., Kutler, J., & Teng-Kui, L. (2006). A Landsat surface reflectance dataset for North America, 1990–2000. *IEEE Geoscience and Remote Sensing Letters*, 3, 68–72.
- Masek, J. G., Huang, C., Cohen, W. B., Kutler, J., Hall, F., & Wolfe, R. E. (2008). Mapping North American forest disturbance from a decadal Landsat record: Methodology and initial results. *Remote Sensing of Environment*, 112, 2914–2926.
- Masek, J.G., Cohen, W.B., Leckie, D., Wulder, M.A., Vargas, R., de Jong, B., Healey, S.P., Law, B., Birdsey, R., Houghton, R.A., Mildrexler, D., Goward, S., and Smith, W.B. (in press). Recent rates of forest harvest and conversion in North America. *Journal of Geophysical Research*.
- McRae, D. J., Duchesne, L. C., Freedman, B., Lynham, T. J., & Woodley, S. (2001). Comparisons between wildfire and forest harvesting and their implications in forest management. *Environmental Review*, 9, 223–260.
- Mildrexler, D. J., Zhao, M., Heinsch, F. A., & Running, S. W. (2007). A new satellite-based methodology for continental-scale disturbance detection. *Ecological Applications*, 17, 235–250.
- Mildrexler, D. J., Zhao, M., & Running, S. W. (2009). Testing a MODIS Global Disturbance Index across North America. *Remote Sensing of Environment*, 113, 2103–2117.
- Mkhabela, M. S., Amiro, B. D., Barr, A. G., Black, T. A., Hawthorne, I., Kidston, J., McCaughey, J. H., Orchansky, A. L., Nestic, Z., Sass, A., Shashkov, A., & Zha, T. (2009). Comparison of carbon dynamics and water use efficiency following fire and harvesting in Canadian boreal forests. *Agricultural and Forest Meteorology*, 149, 783–794.
- Morrison, I. N., & Kraft, D. (1994). Sustainability of Canada's agri-food system – A prairie perspective. *International Institute for Sustainable Development, Winnipeg, MB* 168 pp.
- Niemelä, J. (1999). Management in relation to disturbance in the boreal forest. *Forest Ecology and Management*, 115, 127–134.
- Olsson, H. (1994). Changes in satellite-measured reflectances caused by thinning cuttings in boreal forest. *Remote Sensing of Environment*, 50, 221–230.
- Payette, S. (1992). Fire as a controlling process in the North American boreal forest. In H. H. Shugart, R. Leamans, & G. B. Bonan (Eds.), *A systems analysis of the global boreal forest* (pp. 144–169). Cambridge, UK: Cambridge University Press.
- Peltzer, D. A., Bast, M. L., Wilson, S. D., & Gerry, A. K. (2000). Plant diversity and tree responses following contrasting disturbances in boreal forest. *Forest Ecology and Management*, 127, 191–203.
- Perera, A. H., Buse, L. J., & Weber, M. G. (2004). *Emulating natural forest landscape disturbances: Concepts and applications*. New York, NY: Columbia University Press 352 pp.
- Pinel-Alloul, B., Prepas, E., Planas, D., Steedman, R., & Charette, T. (2002). Watershed impacts of logging and wildfire: Case studies in Canada. *Lake and Reservoir Management*, 18, 307–318.
- Powell, S. L., Cohen, W. B., Healey, S. P., Kennedy, R. E., Moisen, G. G., Pierce, K. B., & Ohmann, J. L. (2010). Quantification of live aboveground forest biomass dynamics with Landsat time series and field inventory data: A comparison of empirical modeling approaches. *Remote Sensing of Environment*, 114, 1053–1068.
- Ranson, K. J., Kovacs, K., Sun, G., & Kharuk, V. I. (2003). Disturbance recognition in the boreal forest using radar and Landsat-7. *Canadian Journal of Remote Sensing*, 29, 271–285.
- Rouse, J. W., Hass, R. H., Schell, J. A., & Deering, D. W. (1973). Monitoring vegetation systems in the Great Plains with ERTS. *3rd ERTS Symposium, NASA SP-351*, 1. (pp. 309–317).
- Roy, D. P., Jin, Y., Lewis, P. E., & Justice, C. O. (2005). Prototyping a global algorithm for systematic fire-affected area mapping using MODIS time series data. *Remote Sensing of Environment*, 97, 137–162.
- Roy, D. P., Boschetti, L., & Trigg, S. N. (2006). Remote sensing of fire severity: Assessing the performance of the normalized burn ratio. *IEEE Geoscience and Remote Sensing Letters*, 3, 112–116.
- Roy, D. P., & Boschetti, L. (2009). Southern Africa validation of the MODIS, L3JRC and GlobCarbon burned-area products. *IEEE Transactions on Geoscience and Remote Sensing*, 47, 1–13.
- Running, S., Peterson, D., Spanner, M., & Teuber, K. (1986). Remote sensing of coniferous forest leaf area. *Ecology*, 67, 273–276.
- Sader, S. A., & Winne, J. C. (1992). RGB-NDVI colour composites for visualizing forest change dynamics. *International Journal of Remote Sensing*, 13, 3055–3067.
- Schroeder, D., & Perera, A. H. (2002). A comparison of large-scale spatial and vegetation patterns following clearcuts and fires in Ontario's boreal forests. *Forest Ecology and Management*, 159, 217–230.
- Schroeder, T. A., Cohen, W. B., Song, C., Canty, M. J., & Yang, Z. (2006). Radiometric correction of multi-temporal Landsat data for characterization of early successional forest patterns in western Oregon. *Remote Sensing of Environment*, 103, 16–26.
- Sellers, P. J., Berry, J. A., Collatz, G. J., Field, C. B., & Hall, F. G. (1992). Canopy reflectance, photosynthesis, and transpiration. III. A reanalysis using improved leaf models and a new canopy integration scheme. *Remote Sensing of Environment*, 42, 187–216.
- Skinner, W. R., Stocks, B. J., Martell, D. L., Bonsal, B., & Shabbar, A. (1999). The association between circulation anomalies in the mid-troposphere and area burned by wildland fire in Canada. *Theoretical and Applied Climatology*, 63, 89–105.
- Stehman, S. V., & Czaplewski, R. L. (1998). Design and analysis for thematic map accuracy assessment: fundamental principles. *Remote Sensing of Environment*, 64, 331–344.
- Stocks, B. J., Mason, J. A., Todd, J. B., Bosch, E. M., Wotton, B. M., Amiro, B. D., Flannigan, M. D., Hirsch, K. G., Logan, K. A., Martell, D. L., & Skinner, W. R. (2003). Large forest fires in Canada 1959–1997. *Journal of Geophysical Research*, 107, 8149.
- Thomas, N. E., Huang, C., Goward, S. N., Powell, S., Rishmawi, K., Schleeuwis, K., & Hinds, A. (2011). Validation of North American Forest Disturbance dynamics derived from Landsat time series stacks. *Remote Sensing of Environment*, 115, 19–32.
- Townshend, J. R., & Justice, C. O. (1988). Selecting the spatial resolution of satellite sensors required for global monitoring of land transformations. *International Journal of Remote Sensing*, 9, 187–236.
- Turner, D. P., Cohen, W. B., Kennedy, R. E., Fassnacht, K. S., & Briggs, J. M. (1999). Relationships between leaf area index and Landsat TM spectral vegetation indices across three temperate zone sites. *Remote Sensing of Environment*, 70, 52–68.
- Verbyla, D. L., Kasischke, E. S., & Hoy, E. E. (2008). Seasonal and topographic effects on estimating fire severity from Landsat TM/ETM+ data. *International Journal of Wildland Fire*, 17, 527–534.
- Weber, M. G., & Flannigan, M. D. (1997). Canadian boreal forest ecosystem structure and function in a changing climate: Impact on fire regimes. *Environmental Review*, 5, 145–166.
- Wilson, E. H., & Sader, S. A. (2002). Detection of forest harvest type using multiple dates of Landsat TM imagery. *Remote Sensing of Environment*, 80, 385–396.
- Woodcock, C. E., Allen, R., Anderson, M., Belward, A., Bindschadler, R., Cohen, W., Gao, F., Goward, S. N., Helder, D., Helmer, E., Nemani, R., Oreopoulos, L., Schott, J., Thenkabail, P. S., Vermote, E. F., Vogelmann, J., Wulder, M. A., & Wynne, R. (2008). Free access to Landsat imagery. *Science*, 320(5879), 1011.
- Wulder, M. A., Skakun, R. S., Dymond, C. C., Kurz, W. A., & White, J. C. (2005). Characterization of the diminishing accuracy in detecting forest insect damage over time. *Canadian Journal of Remote Sensing*, 31, 421–431.
- Wulder, M. A., Campbell, C., White, J. C., Flannigan, M., & Campbell, I. D. (2007). National context in the international circumboreal community. *The Forestry Chronicle*, 83, 539–556.
- Wulder, M. A., White, J. C., Goward, S. N., Masek, J. G., Irons, J. R., Herold, M., Cohen, W. B., Loveland, T. R., & Woodcock, C. E. (2008). Landsat continuity: Issues and opportunities for land cover monitoring. *Remote Sensing of Environment*, 112, 955–969.
- Wulder, M. A., White, J. C., Gillis, M. D., Walsworth, N., Hansen, M. C., & Potapov, P. (2009a). Multi-scale satellite and spatial information and analysis framework in support of a large-area forest monitoring and inventory update. *Environmental Monitoring and Assessment*, doi:10.1007/s10661-009-1243-8 Open Access. <http://www.springerlink.com/content/4652210u416431x8/>.
- Wulder, M. A., White, J. C., Alvarez, F., Han, T., Rogan, J., & Hawkes, B. (2009b). Characterizing boreal forest wildfire with multi-temporal Landsat and LIDAR data. *Remote Sensing of Environment*, 113, 1540–1555.
- Zhang, Q., & Chen, W. (2007). Fire cycle of the Canada's boreal region and its potential response to global climate. *Journal of Forestry Research*, 18, 55–61.